Morphogenesis of Liposomes Caused by Polycation-Induced Actin Assembly Formation

Haruka Maemichi, Kazuhiro Shikinaka, Akira Kakugo, Hidemitsu Furukawa, Yoshihito Osada,† and Jian Ping Gong*

Department of Biological Sciences, Graduate School of Science, Hokkaido University, Sapporo 060-0810, Japan

Received July 1, 2008. Revised Manuscript Received August 12, 2008

We investigated the effects of polycation-mediated actin assembly on the morphological transformation of the lipid vesicle membrane by spatiotemporally controlling actin assembly. By triggering the radical polymerization of the cationic monomer using UV irradiation, we achieved a varied photoinduced assembly of actin in bulk solution. Furthermore, we designed liposomes containing actin and cationic monomers. In these actin-encapsulated liposomes, various actin assemblies were formed by UV irradiation similar to that observed in bulk solution. Moreover, morphogenesis of actin-encapsulated liposomes was observed in liposomes encapsulated with G-actin but not with F-actin. This result indicates that a dynamic polymerization of G-actin is important for vesicle protrusion.

Introduction

Actin, which is a globular protein, is one of the most abundant proteins present in all eukaryotic cells. Not only does it provide the cell with a high mechanical strength, but it also facilitates cell movement processes such as cytokinesis, cell crawling, cytoplasmic streaming, and muscle contraction.[1] Actin exhibits various morphologies in vivo depending on specific actin-related linker proteins.[2] The polymorphism of actin is considered to be responsible for its multifunctionality. Recently, it has been demonstrated that the morphology of actin assembly is determined not only by specific linker proteins but also by other factors such as the concentration of linker proteins, environmental conditions (ionic strength or pH), and the kinetics of actin−linker protein interactions.[3−6]

Actin monomer (G-actin) has an intrinsic binding site for end-to-end annealing to form a filamentous assembly termed F-actin. Under physiological conditions, F-actin behaves like a negatively charged rigid rod.[7] F-actins can also assemble into diverse morphologies through electrostatic interaction with multivalent cations or polycations in vitro.[8−13] For example, we have reported that F-actins form bundles with poly-L-lysine and the poly-*N*-[3-(dimethylamino)propyl]acrylamide methyl chloride quaternary (PDMAPAA-Q) compound. In these studies, it has been revealed that the thickness (D) of the actin bundle is determined by the polycation-mediated attraction between F-actins and the length (L) of the actin bundle is influenced by the actin concentration (C_A).[14−16] Various growth phenomenon of actin bundles formed with polymer or actin-related linker protein have also been reported by other researchers,[17−19] and the results of these reports are well in agreement with those of our studies. Thus far, the above-described assembly has mostly been performed in bulk solutions. Under natural conditions, such as in cells, the reaction space is surrounded by a lipid vesicle and its dimension is of the order of the persistence length of F-actins, approximately 10 μm. This confined space would influence not only the morphological transformation of the vesicle but also structural change in the actin assembly.[20] In this paper, we investigate the effect of polycation-mediated actin assembly on the morphological transformation of the lipid vesicle membrane. Thus far, it has been revealed that F-actin is unable to cause vesicle protrusions unless bundled with actin-related linker proteins to gain sufficient rigidity.[21] Our previous studies have shown that the actin assembly is approximately 30−60 nm thick when formed with polycations;[15] this is several times thicker than that of F-actin. Since bending rigidity increases with thickness D, varying as D^4,[14,22] it is assumed that polycation-mediated actin assembly is strong enough to cause vesicle protrusion.

* Corresponding author. E-mail: gong@sci.hokudai.ac.jp.
† Present address: Riken, Saitama 351-0198, Japan.

(1) Bray, D. *Cell Movements from Molecules to Motility*, 2nd ed.; Garland Publishing: London, U.K., 2001.
(2) Lodish, H.; Berk, A.; Kaiser, C. A.; Krieger, M.; Scott, M. P.; Bretscher, A.; Ploegh, H.; Matsudaira, P. T. *Molecular Cell Biology*, 4th ed.; W. H. Freeman & Co. Ltd.: San Francisco, CA, 1999.
(3) DeRosier, D. J.; Tilney, L. G. *J. Cell Biol.* **2000**, *148*, 1–6.
(4) Meyer, R. K.; Aebi, U. *J. Cell Biol.* **1990**, *110*, 2013–2024.
(5) Pelletier, O.; Pokidysheva, E.; Hirst, L. S.; Bouxsein, N.; Li, Y.; Safinya, C. R. *Phys. Rev. Lett.* **2003**, *91*, 148102.
(6) Tseng, Y.; Fedorov, E.; McCaffery, J. M.; Almo, S. C.; Wirtz, D. *J. Mol. Biol.* **2001**, *310*, 351–366.
(7) Yanagida, T.; Nakase, M.; Nishiyama, K.; Oosawa, F. *Nature* **1984**, *307*, 58–60.
(8) Tang, J. X.; Wong, S.; Tran, P.; Janmey, P. A. *Ber. Bunsen-Ges.* **1996**, *100*, 796–806.
(9) Lai, G. H.; Coridan, R.; Zribi, O. V.; Golestanian, R.; Wong, G. C. L. *Phys. Rev. Lett.* **2007**, *98*, 187802.
(10) Tang, J. X.; Janmey, P. A. *J. Biol. Chem.* **1996**, *271*, 8556–8563.
(11) Tang, J. X.; Ito, T.; Tao, T.; Traub, P.; Janmey, P. A. *Biochemistry* **1997**, *36*, 12600–12607.
(12) Kakugo, A.; Sugimoto, S.; Gong, J. P.; Osada, Y. *Adv. Mater.* **2002**, *14*, 1124–1126.
(13) Kakugo, A.; Shikinaka, K.; Matsumoto, K.; Gong, J. P.; Osada, Y. *Bioconjugate Chem.* **2003**, *14*, 1185–1190.
(14) Kwon, H. J.; Kakugo, A.; Shikinaka, K.; Osada, Y.; Gong, J. P. *Biomacromolecules* **2005**, *6*, 3005–3009.
(15) Kwon, H. J.; Tanaka, Y.; Kakugo, A.; Shikinaka, K.; Furukawa, H.; Osada, Y.; Gong, J. P. *Biochemistry* **2006**, *45*, 10313–10318.
(16) Shikinaka, K.; Kwon, H. J.; Kakugo, A.; Furukawa, H.; Osada, Y.; Gong, J. P.; Aoyama, Y.; Nishioka, H.; Jinnai, H.; Okajima, T. *Biomacromolecules* **2008**, *9*, 537–542.
(17) Haviv, L.; Gov, N.; Ideses, Y.; Bernheim-Groswasser, A. *Eur. Biophys. J.* **2008**, *37*, 447–454.
(18) Popp, D.; Gov, N. S.; Iwasa, M.; Maeda, Y. *Biopolymers* **2008**, *89*, 711–721.
(19) Grason, G. M.; Bruinsma, R. F. *Phys. Rev. Let.* **2007**, *99*, 098101.
(20) Miyata, H.; Hotani, H. *Proc. Natl. Acad. Sci. U.S.A.* **1992**, *89*, 11547–11551.
(21) Honda, M.; Takiguchi, K.; Ishikawa, S.; Hotani, H. *J. Mol. Biol.* **1999**, *287*, 293–300.
(22) Howard, J. *Mechanics of Motor Proteins and the Cytoskeleton*; Sinauer Associates Inc.: Sunderland, MA, 2001; pp 100−116..

10.1021/la802057c CCC: $40.75
Published on Web 09/12/2008

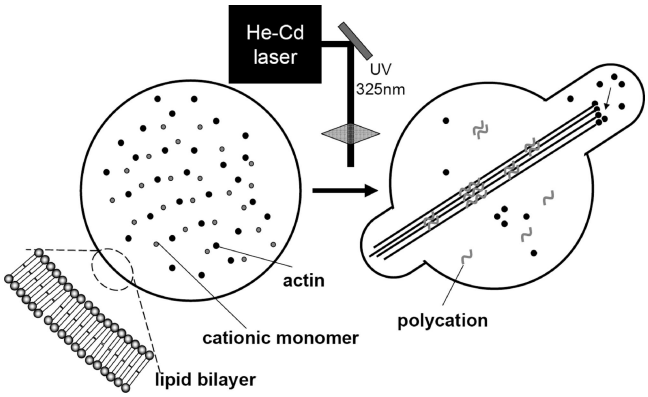

Figure 1. Scheme of photoinduced actin assembly formation in liposome.

In this study, the liposome comprised a lipid bilayer membrane and the PDMAPAA-Q compound used as the vesicle and polycation, respectively. In order to spatiotemporally control the self-assembly process, we use the following strategy as illustrated in Figure 1: (1) encapsulate actins and the DMAPAA-Q cation monomers in the liposome, (2) initiate the polymerization of DMAPAA-Q by UV irradiation, and (3) observe the morphogenesis of liposome, caused by actin assembly.

In order to realize this strategy, we first investigated the photoinduced actin bundle formation process in bulk solution by using a UV irradiation system consisting of an optical lens and a fiber. The actin and cation monomers were then encapsulated in a liposome, and morphogenesis of the liposome was characterized after UV irradiation. Actins and cationic monomers were encapsulated in the liposome by using the hydration method described in a published paper.[23] Assembly formation of the encapsulated actins was spatiotemporally controlled using the UV irradiation system to lead to the polymerization of cationic monomers (DMAPAA-Q).

Here, we demonstrate that assembly of various sizes and shapes of actin depending on DMAPAA-Q monomer concentration (C_M) and radical initiator concentration (R_I) can be induced by UV irradiation in a bulk solution. Further, we reported that PDMAPAA-Q-mediated actin assembly can deform the liposome membrane. We also discuss the importance of the dynamic polymerization of actin.

Materials and Methods

Sample Preparations. *Actin Preparation.* G-actin was purified from scallops by using the method of Spudich and Watt.[24] Fluorescence-labeled G-actin was obtained as follows: filamentous actin was prepared by polymerization of G-actin for 60 min in F-buffer (5 mM HEPES (pH 7.2), 0.2 mM ATP, 0.2 mM $CaCl_2$, 0.1 M KCl, 2 mM $MgCl_2$). We mixed this F-actin with 5- and 6-carboxytetrametylrhodamine, succinimidyl ester (TAMRA-SE, C-1171, Invitrogen) for 30 min at 37 °C. The samples were then centrifuged at 62 000 rpm for 30 min (Hitachi ultracentrifuge, Himac CP70MX; rotor, R65A) to obtain the stained F-actin. The resultant pellet containing stained F-actin was diluted with G-buffer (5 mM HEPES (pH 7.2), 0.2 mM ATP, 0.2 mM $CaCl_2$, and 2 mM $MgCl_2$) to depolymerize F-actin to G-actin, and it was then stored at 4 °C. The labeling ratio of fluorescence dye to G-actin was 0.12 [mol/mol], which was determined by measuring the absorbance of the protein at 280 nm and that of tetramethylrhodamine at 555 nm for TAMRA-SE and Alexa 488 SE.

Fluorescence-labeled filamentous actin was obtained by mixing G-actin (23.2 μM) with rhodamine−phalloidin (Molecular Probes No. 4171) (0.129 μM) in F-buffer for 24 h at 4 °C. Phalloidin stoichiometrically binds to G-actin and stabilizes F-actin against depolymerization at low G-actin concentrations. To allow the clear visualization of F-actin at high concentrations (1 mg/mL), it was labeled with a very small amount of rhodamine−phalloidin.

Reagents. We used the *N*-[3-(dimethylamino)propyl]acrylamide methyl chloride quaternary (DMAPAA-Q; Tokyo Kasei Co., Ltd.) compound as a cationic monomer and 2-oxoglutaric acid (Wako Pure Chemical Industries, Ltd.) as a radical initiator. 1,2-Dimyristoyl-*sn*-glycero-3-[phospho-*rac*-(1-glycerol)] (sodium salt) (DMPG) was purchased from Wako Pure Chemical Industries, Ltd. L-α-Phosphatidylcholine (PC) from chicken egg was purchased from Jena Bioscience (Germany).

Experiments. *Preparation of Reaction Mixture.* The reaction mixture was prepared by mixing DMAPAA-Q, 2-oxoglutaric acid, KCl, and actin (G- or F-form) in G-buffer. The actin concentration C_A, expressed in terms of the G-actin concentration, was kept constant at 1 mg/mL (corresponding to 23.2 μM). The DMAPAA-Q concentration C_M was varied from 10^{-4} to 0.6 M. The 2-oxoglutaric acid ratio R_I was varied from 0.1 to 2 mol % (the molar percentages are with respect to the DMAPAA-Q monomer). The KCl concentration C_S was kept constant at 50 mM.

Preparation of Actin-Encapsulated Liposome. Actin-encapsulated liposomes were prepared using the hydration method reported by Bangham and Horne.[23] In a test tube, 150 μL of 0.967 mM DMPG and 2.63 mM phospholipids in chloroform and methanol were placed, and the mixture was dried by a steam of argon gas at room temperature. The residual solvent was completely removed by a rotary vacuum pump for more than 5 h, and a dried lipid film was produced in the test tube. Small aliquots of reaction mixtures (2 μL) were added to the test tube and incubated at room temperature for a few minutes (prehydration). The actin-encapsulated liposome was then obtained upon swelling of the dried lipid film in 100 μL of the reaction mixture at room temperature. For the control experiment, liposomes containing no actin were also prepared by the same method. The unilamellarity of liposome was examined by optical microscope observation with visual judgment.

Photoinduced Actin Assembly Formation. A cover glass was placed on a slide glass equipped with silicon spacers (approximately 0.2 mm in height) on either side to form a cell. The reaction mixture (approximately 10 μL) was introduced into the cell by a micropipette. UV light at 325 nm was irradiated through optical fiber (Newport Corporation) to the cell from the top of the cover glass for 30 min by He−Cd laser (Kimmon Koha Co., Ltd.) with a collective and objective lens (under atmospheric conditions), to produce an illumination spot of approximately 20 mm^2.

Observations. *Fluorescence Microscopy (FM).* The cell containing the actin assembly was placed on the stage of a fluorescence microscope (Olympus BX 50) and observed under a 60× objective lens. The fluorescence images were recorded by a CCD camera (Olympus CD-300T-RC).

Transmission Electron Microscopy (TEM). TEM was performed by using a JEM-1200EX (JEOL Ltd., Tokyo, Japan) at an acceleration voltage of 80 kV. The sample (10 μL) was dropped on carbon-coated grids (Nisshin EM Co., Tokyo), which were rendered hydrophilic by glow charge under reduced pressure. After 3 min on the grids, 2% (w/v) uranyl acetate was added to the sample and the grids were air-dried. The average thickness (D) of the actin bundle was obtained from 20 samples.

Estimation of Actin Concentration in Liposomes. The actin concentration in liposome was estimated from a fluorescent intensity, which was measured by confocal laser scanning microscopy (CLSM; FV 200, Olympus) at room temperature. Excitation was performed at $\lambda = 480$ nm, and observations were made at $\lambda = 520$ nm, with a slit width of 100 μm. The actin solution at various C_A values (0.25, 0.5, 0.75, and 1 mg/mL) and buffer solution without actin were used for plotting the standard curve.

(23) Bangham, A. D.; Horne, R. W. *J. Mol. Biol.* **1964**, *8*, 660–668.
(24) Spudich, J. A.; Watt, S. *J. Biol. Chem.* **1971**, *246*, 4866–4871.

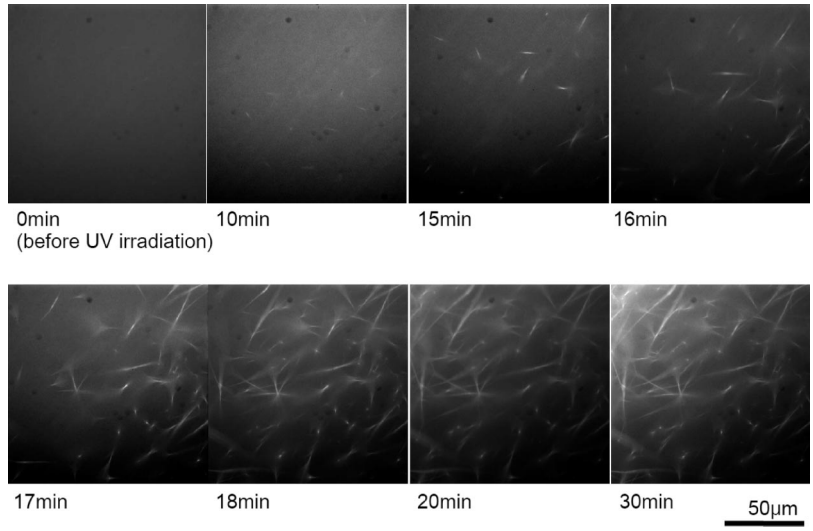

Figure 2. Fluorescence images of time evolution of actin assembly formation by UV irradiation at $C_M = 0.4$ M and $R_I = 2$ mol %. The scale bar represents 50 μm.

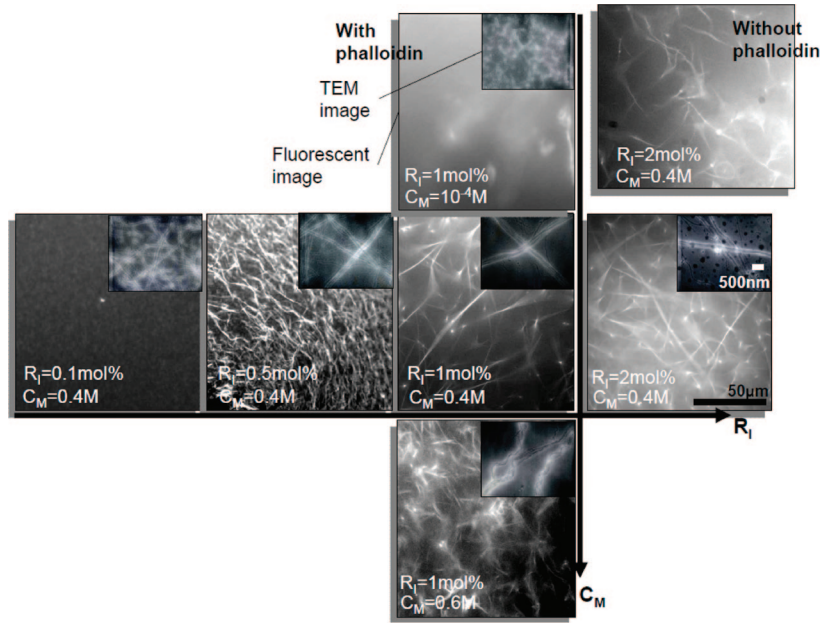

Figure 3. Fluorescence and TEM images (insets) of the actin assemblies formed in various C_M and R_I values in the presence of phalloidin after 30 min of UV irradiation. A fluorescence image of the actin assemblies formed at $C_M = 0.4$ M and $R_I = 2$ mol % in the absence of phalloidin is shown in the upper right corner. Scale bars in the fluorescence and TEM images represent 50 μm and 500 nm, respectively.

Results and Discussion

Photoinduced Actin Assembly Formation in Bulk Solution. Prior to study the assembly formation of the encapsulated actins, we investigated the assembly formation induced by UV irradiation in the bulk solution. The 0 min image in Figure 2 illustrates the fluorescence image of actins in the reaction mixture before UV irradiation. The reaction mixture contains cationic monomers and radical initiators. As illustrated in this figure, at the concentration of 1 mg/mL, actins are present as single filaments (F-actin), 1−5 μm in length (since the magnification is low, F-actins cannot be seen in this figure). After 15 min of UV irradiation at 325 nm, the F-actins began to assemble and continue to grow and form a giant network assembly after 30 min (Figure 2).

Next, we investigated the effect of cationic monomer (DMAPAA-Q) concentrations (C_M) and the radical initiator concentration (R_I). Figure 3 illustrates the fluorescence and TEM images of the actin assemblies with phalloidin after 30 min of UV irradiation with various DMAPAA-Q concentration (C_M) and radical initiator concentration (R_I). The horizontal row in Figure 3 exhibits the effect of R_I on the actin assembly at a constant C_M of 0.4 M. When the C_M was kept constant and the R_I value was varied, F-actins formed a giant network above the R_I value of 0.5 mol %. Then, R_I was maintained at 1 mol % (relative to the DMAPAA-Q monomer) and the value of C_M was varied from 10^{-4} to 0.6 M. At $C_M = 10^{-4}$ M and $R_I = 1$ mol %, F-actins formed small aggregations, but bundle formation was not observed. In the C_M range from 0.001 to 0.3 M, small actin assembly was unexpectedly observed before UV irradiation. This might by due to the presence of DMAPAA-Q oligomers, since DMAPAA-Q was used as purchased without a further purifi-

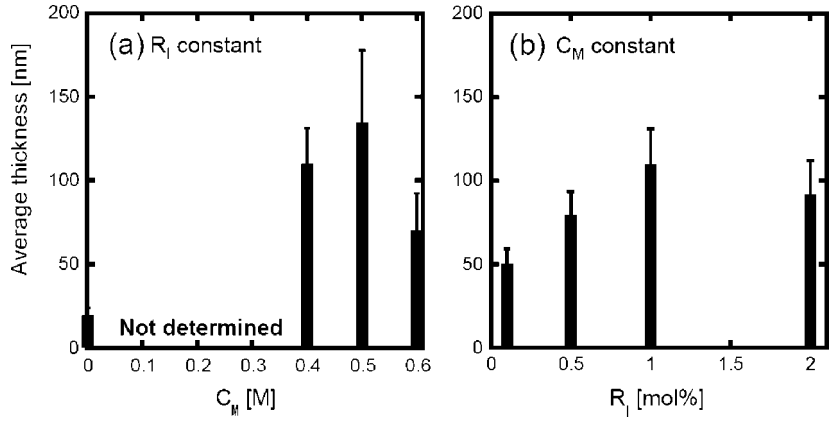

Figure 4. Average thickness D of the actin bundles formed at various C_M values with a constant R_I value of 1 mol % (a) and at various R_I values with a constant C_M value of 0.4 M (b).

cation. At $C_M = 0.4$ M, giant actin assembly network was observed. When $C_M = 0.6$ M, the assembly becomes thin and weak.

Let us discuss the various morphology depending on C_M and R_I. In our previous paper,[15] we studied the effect of electrostatic interactions on the size and morphology of actin bundles by regulating the poly-L-lysine concentration (C_P), polymerization degree (N) of poly-L-lysine, and KCl salt concentration (C_S). We revealed that the average thickness (D) of actin bundles tends to increase with decreasing N and that the increase in C_P favors the nucleation and increases the nuclei concentration (C_N). On the other hand, an increase in C_S leads to an increased D value due to screening of the electrostatic interaction. The larger the N, the greater is the entropy gain by binding due to counterion release. The critical polycation concentration for inducing bundle formation (C^C_P) decreases dramatically with an increase in N. In this study, the N value of the polymerized PDMAPAA-Q was changed by R_I at a constant C_M. Increasing the R_I value led to an increase in the initiation site, which led to a decrease in the polycation N value.[25] Similarly, the C_P value increased when the C_M value was increased and the R_I value was kept constant.

The density of actin network decreases with an increase in R_I at constant C_M as shown in Figure 3. The N of the polymerized PDMAPAA-Q would decrease with an increase in R_I. On the other hand, the C^C_P increases with the decrease in the N, and the D increases with the decrease in N.[15] This explains the phenomenon of a decreased density of actin network assemblies with increasing R_I. The morphological change of actin assemblies with increasing C_M from 0.4 to 0.6 M should be attributed to the increase in C_N due to increasing C_P with C_M.

The upper right image in Figure 3 also displays the fluorescence image of actin assemblies without phalloidin after 30 min of UV irradiation at $C_M = 0.4$ M and $R_I = 2$ mol %. No distinct differences between actin assemblies formed with and without phalloidin are detected in the fluorescence image.

TEM images (insets) reveal that the actin network consists of crossovers and branches of actin bundles (Figure 3). The average thickness D of the actin bundles in the assembly at various C_M and R_I values is summarized in Figure 4. At the constant R_I value of 1 mol %, the D of the actin bundle increases with in the C_M range from 0.4 to 0.5 M. On the other hand, the D value decreases with increase in the C_M value from 0.5 to 0.6 M. The excessive addition of cation induces positive overcharging to the F-actin,[13] which should cause the bundles to disassemble. These morphological change depending on the C_M was also observed in the previous system in which actin bundle was formed by simply mixing with polycation.[14] Meanwhile, at a constant C_M of 0.4 M, the D of bundle increases with increasing R_I until $R_I = 1$ mol %, and it remains nearly constant above the $R_I = 1$ mol %. This could be explained by the decrease in N due to an increase in R_I, which weakens the electrostatic attraction between the actin and polycations. In a previous study, increase of the D with decrease in the N was observed in the actin and poly-L-lysine system;[15] this tendency is well in agreement with the presented study.

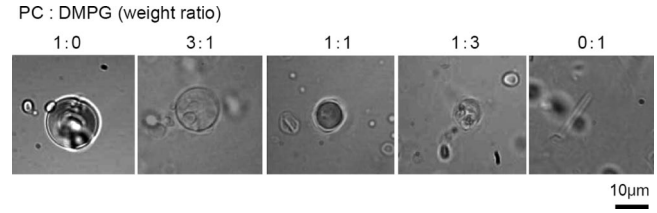

Figure 5. Optical microscope images of actin-encapsulated liposomes formed at various ratios of PC to DMPG. The scale bar represents 10 μm.

Thus far, it has been revealed that F-actin is unable to cause vesicle protrusions unless bundled with actin-related linker proteins to gain sufficient rigidity.[16] The D of the actin assembly is approximately 50−130 nm, which is several times thicker than F-actin. Since rigidity increases with thickness D, varying as D^4,[14,22] it is assumed that polycation-mediated actin assembly is strong enough to cause vesicle protrusion.

Preparation of Actin-Encapsulated Liposomes. We employed the hydration method to encapsulate actins within liposomes (refer to the Experiments section). In this experiment, photoinduced actin assembly is performed in the reaction mixture containing 0.4 M cationic monomer and 2 mol % radical initiator. Usually, in such a high ionic concentration, liposome formation is difficult.[26] To find the optimized condition to encapsulate the actins, we surveyed various lipid compositions consist of neutral (PC) and basic (DMPG) phospholipids. Figure 5 illustrates the optical microscope images of liposomes formed with various ratios of PC and DMPG. When PC/DMPG is 1:0, 1:1, 1:3, and 0:1, multilamellar liposomes without encapsulating actins with phalloidin were observed; this was confirmed with FM. In contrast, unilamellar liposomes were observed with encapsulating actins when the PC/DMPG ratio was 3:1. This indicates that electrostatic

(25) Flory, P. J. *Principle of Polymer Chemistry*; Cornell University Press: New York, 1953.

(26) Yamashita, Y.; Oka, M.; Tanaka, T.; Yamazaki, M. *Biochem. Biophys. Acta* **2002**, *1561*, 129–134.

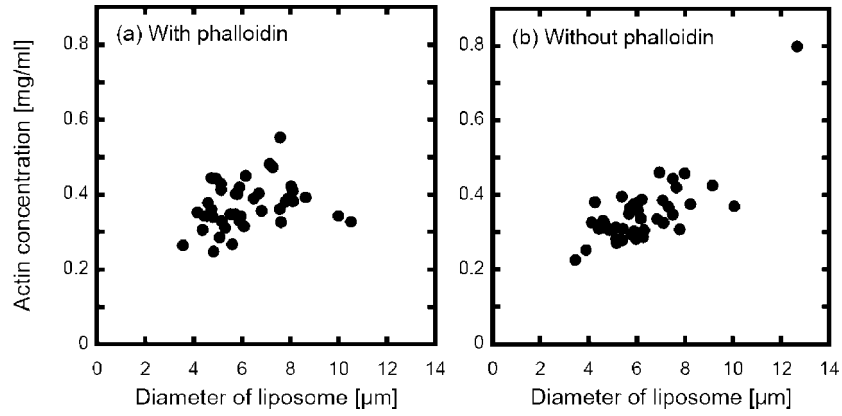

Figure 6. Liposome diameter dependence of actin concentration encapsulated in liposome for actin solution with (a) and without (b) phalloidin. The C_M and R_I of the actin solution are 0.4 M, and 2 mol %, respectively. The ratio of PC/DMPG is 3:1.

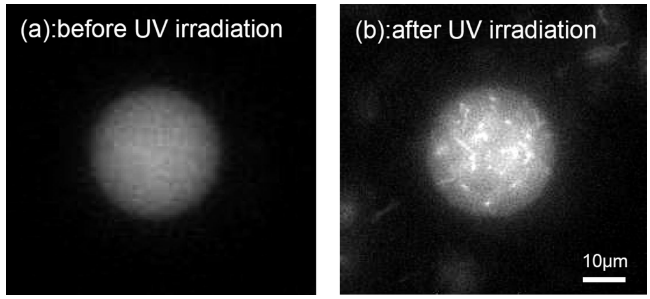

Figure 7. Fluorescence images of actin with phalloidin encapsulated in liposome before (a) and after (b) 30 min of UV irradiation. The C_M and R_I of the actin solution are 0.4 M, and 2 mol %, respectively. The ratio of PC/DMPG is 3:1. The scale bar represents 10 μm.

repulsion between basic lipids may be required to form unilamellar liposomes; however, the detailed mechanism is still unclear.

Relationship between the actin concentration in liposome and the liposome size is illustrated in Figure 6. As shown in this figure, there is no difference in the actin concentration for the liposome size with or without phalloidin.

Morphogenesis of Actin-Encapsulated Liposomes. Figure 7a illustrates the fluorescence images of actin encapsulated in the liposome. Phalloidin (0.129 μM), which is a reagent inhibiting F-actin disassembly, was also encapsulated in the liposome. Actin assembly in the liposome was observed when the actin-encapsulated liposome was irradiated with UV at 325 nm for 30 min (Figure 7b).

Figure 8a illustrates fluorescence images of F-actin-encapsulated liposomes of sizes ranging from 2 to 20 μm, after UV irradiation for 30 min. As shown in this figure, the morphology of actin assembly changes depending on the size of the liposome. When the diameter of the liposome is smaller than 5 μm, F-actins form a ring-shaped assembly along the liposome periphery (Figure 8a-1). In contrast, in liposomes with sizes larger than 5 μm in diameter, F-actin forms a network assembly (Figure 8, parts a-2, a-3, and a-4). This structural transformation of actin assembly from ring to network depending on the diameter of the liposome was also observed in F-actin/α-actinin assemblies formed in liposomes.[27] Unfortunately, despite the bundle or network formation of F-actins, no liposome transformation or protrusion was observed.

Fluorescence images of liposome-encapsulated actin without phalloidin are illustrated in Figure 8b after UV irradiation for 30 min. Different from the F-actin-encapsulated liposome, not

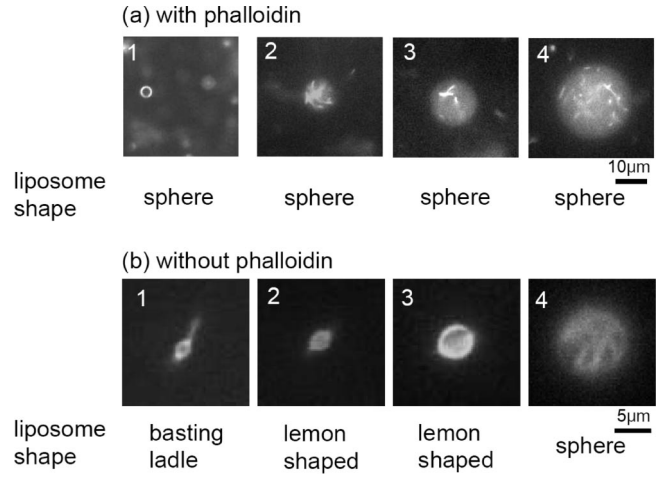

Figure 8. Various morphogenesis of liposome encapsulating actin with (a) and without phalloidin (b) after UV irradiation at 325 nm for 30 min. The C_M and R_I values of the actin solution are 0.4 M and 2 mol %, respectively. The ratio of PC/DMPG is 3:1. The scale bar represents 10 μm.

only the morphological changes of actin assembly but also liposome transformation depending on liposome diameter is observed. When the liposome diameter is approximately 2−3 μm, actin forms a bundle, and the liposome is transformed into basting ladle-shaped structure (Figure 8b-1). When the liposome diameter is approximately 3−5 μm, the actin forms a bundle and the liposome is transformed into a lemon-shaped structure (Figure 8, parts b-2 and b-3). These behaviors are considerably similar to those observed in liposomes containing actin and actin-binding proteins.[20] When the diameter of liposome is larger than 5 μm, actins form a network and the liposome maintains the spherical shape as in the case of actin-encapsulated liposomes with phalloidin (Figure 8b-4).

It is known that a transformation of liposome is driven by change of osmotic pressure, and consequently, they transform into various shapes.[28] Transformation of the actin-encapsulated liposomes here is driven by actin assembly, which is confirmed by the fact that the liposomes in the reaction mixture do not transform before and after UV irradiation in the absence of actin (Figure 9).

By other group, the dependence of vesicle shape deformed by inner filaments on the filament length (L) were simulated.[29] According to this simulation, vesicle shape depends on L if the

(27) Limozin, L.; Sackmann, E. *Phys. Rev. Lett.* **2002**, *89*, 168103.

(28) Hotani, H. *J. Mol. Biol.* **1984**, *178*, 113–120.

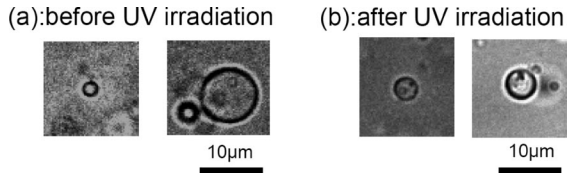

Figure 9. Optical microscope images of the liposomes encapsulating the reaction mixture without actin before (a) and after (b) 30 min of UV irradiation. The C_M and R_I of the solution are 0.4 M, and 2 mol %, respectively. The ratio of PC/DMPG is 3:1. The scale bar represents 10 μm.

diameter of the vesicle and the width of the inner filament are constant, and it has been proposed that there is a threshold of filament length for providing tether initiation (L_1) and giving a vesicle of two-tether shape (L_2). When $L_1 < L < L_2$, the transformation of the spherical vesicle into a basting ladle-shaped vesicle, which has one tether, occurred. Furthermore, when L was smaller than L_1 and larger than the diameter of the vesicle, the vesicle deforms from spherical shape into lemon shape, which is a shape extended one directional. These results indicate that the vesicle shape is transformed from basting ladle shape to lemon shape with an increase in vesicle diameter if the length and width of the inner filament are constant, and the various morphogeneses in our experimental system (Figure 8b) might also be due to the diameter of the liposome and the size of the actin assembly.

In this study, we discuss why liposome morphogenesis into various forms occurs only in encapsulated vesicles in a phalloidin-free actin solution. In the absence of phalloidin, there is a dynamic polymerization and depolymerization of G-actin. The length of filament actin is the result of this dynamic equilibrium, and bundle formation is via G-actin. When the liposome size is comparable to that of the actin bundle, the binding end of the actin filament is located on the inner surface of the liposome. The liposome membrane then undergoes Brownian motion. According to the Brownian ratchet model,[30] the force to deform the membrane is generated by the polymerization of actin. The force generated by the polymerization of actin (F) is determined by the following equation:[22]

$$F = \frac{kT}{\delta} \ln \frac{[A_I]}{K_C}$$

where δ is the increase in length due to incorporation of 1 actin, K_C is the critical concentration for inducing actin polymerization, and $[A_I]$ is the actin concentration (refer to Figure 10). This equation suggests that increase in δ leads to a decrease in the F value. Therefore, the size of δ would influence the difference in the morphogenesis of the vesicle. G-actin, which is actin monomer, is small (5 nm); therefore this would allow it to push and deform the liposome membrane. However, in the presence of phalloidin, the depolymerization of F-actin to G-actin is inhibited; that is, the actin assembly formation is through binding between F-actins directly. F-actin (approximately 1−3 μm) is too large to generate a force that would be sufficient to deform the liposome membrane; thus, the transformation of liposome encapsulated with F-actin cannot occur. This suggests that the dynamic polymerization of G-actin is important for liposome morphogenesis.

To confirm that actin assembly is formed via G-actin without phalloidin while the assembly is formed via F-actin with

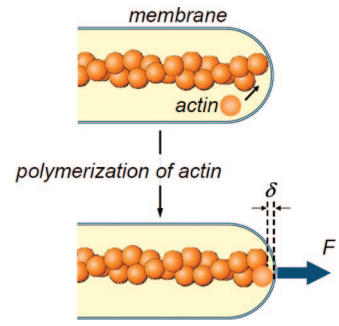

Figure 10. Schematic illustration of the membrane deformation by the polymerization of actin.

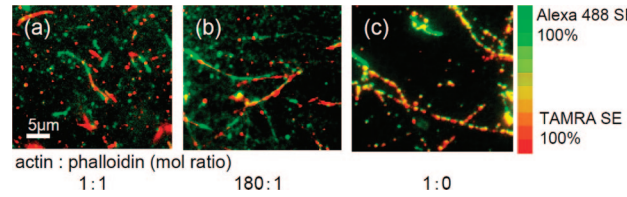

Figure 11. Actin assemblies formed in bulk solution at $C_M = 0.4$ M and $R_I = 2$ mol % with (b) and without (c) phalloidin. As a reference, the ratio of actin/phalloidin = 1:1 is illustrated in (a).

phalloidin, we mixed equal amounts of red- (TAMRA-SE) and green (Alexa-SE)-labeled actins in the reaction mixture with (Figure 11, parts a and b) or without phalloidin (Figure 11c). Prior to mixing the red and green actins, they were separately prepared in the reaction mixture.

Distinct red and green segments are observed when assemblies were formed in the presence of phalloidin (Figure 11, parts a and b), and an average segment length observed in Figure 11b was approximately 4 μm. In contrast, yellow segments indicating the colocalization of the red and green actins were predominantly observed when the assemblies were formed in the absence of phalloidin (Figure 11c). This indicates that, in the absence of the phalloidin, actin assembly is formed via G-actin, whereas in the presence of the phalloidin, actins were incorporated into the assembly as F-actin.

Thus, we have successfully triggered assembly formation of actin in various sizes and shapes, depending on C_M and R_I, by using UV irradiation in a bulk solution. Through this approach, we achieved photoinduced actin assembly formation in liposomes. We found that transformation of the liposome membrane was only observed when actins were encapsulated in the liposome without phalloidin. The dynamic morphological change of cells may be caused by the same actin polymerization and depolymerization mechanism.[31−33] This result suggests that the dynamic polymerization of G-actin at leading edge of actin assembly is important for the morphogenesis of lipid membranes.

Within cells, in order to perform various cellular functions, the structure and the dynamics of the actin bundle and network are spatially regulated through the localization of actin-binding proteins and temporally regulated through coupling of these binding proteins to signal molecules.[31−33] Recently, we found that F-actins effectively assemble into a globally linked network under the unidirectional diffusion of polycations by using a microchamber or polymer gel, even at a dilute actin concentra-

(29) Lim, G. H. W.; Huber, G.; Torii, Y.; Hirata, A.; Miller, J.; Sazer, S. *PLoS ONE* **2007**, *9*, e948.
(30) Peskin, C. S.; Odell, G. M.; Oster, G. F. *Biophys. J.* **1993**, *65*, 316–324.
(31) Chung, C. Y.; Funamoto, S.; Firtel, R. *Trends. Biochem. Sci.* **2001**, *26*, 557–566.
(32) Kurokawa, K.; Nakamura, T.; Aoki, K.; Matsuda, M. *Biochem. Soc. Trans.* **2005**, *33*, 631–634.
(33) Svitkina, T.; Borisy, G. *J. Cell. Biol.* **1999**, *145*, 1009–1026.

tion.[34] This finding indicates that asymmetric distribution or localized activation is essential for organizing actin architectures. To date, many studies on the actin organization have been reported to elucidate the cellular mechanism. However, limited attempts have been made to investigate the effect of spatial distribution of binding proteins or polycations on the actin organization.[35] As a future study, we will investigate the effect of spatial distribution of polycations on the morphological transformation of the actin-encapsulated liposome by applying local UV irradiation.

Acknowledgment. This research is financially supported by the Solution Oriented Research for Science and Technology (SORST) program, Japan Science and Technology Agency (JST), and by the Ministry of Education, Science, Sports and Culture, Japan (Grant-in-Aid for Specially Promoted Scientific Research). We are grateful to Dr. Kingo Takiguchi for his advice.

LA802057C

(34) Kwon, H. J.; Kakugo, A.; Ura, T.; Okajima, T.; Tanaka, Y.; Furukawa, H.; Osada, Y.; Gong, J. P. *Langmuir* **2007**, *23*, 6257–6262.

(35) Misu, M.; Furukawa, H.; Kwon, H. J.; Shikinaka, K.; Kakugo, A.; Satoh, T.; Gong, J. P.; Osada, Y. *J. Biomed. Mater. Res., Part A*, in press.